DOI: 10.3901/CJME.2012.02.328, available online at www.springerlink.com; www.cjmenet.com; www.cjmenet.com.cn

Geometry Design and Tooth Contact Analysis of Crossed Beveloid Gears for Marine Transmissions

ZHU Caichao[1], SONG Chaosheng[1, *], LIM Teik Chin[1, 2], and VIJAYAKAR Sandeep[3]

1 *State Key Laboratory of Mechanical Transmission, Chongqing University, Chongqing 400030, China*
2 *School of Dynamics Systems at University of Cincinnati, Cincinnati, Ohio 45221, USA*
3 *Advanced Numerical Solutions, 3956 Brown Park Drive, Suite B, Hilliard, Ohio 43026, USA*

Received November 17, 2010; revised April 19, 2011; accepted May 3, 2011

Abstract: Beveloid gears, also known as conical gears, gain more and more importance in industry practice due to their abilities for power transmission between parallel, intersected and crossed axis. However, this type of gearing with crossed axes has no common plane of action which results in a point contact and low tooth durability. Therefore, a geometry design approach assuming line contact is developed to analyze the tooth engagement process of crossed beveloid gears with small shaft angle for marine transmission applications. The loaded gear tooth contact behavior is simulated by applying a quasi-static analysis to study the effects of gearing parameters on mesh characteristics. Using the proposed method, a series of sensitivity analyses to examine the effects of critical gearing parameters such as shaft angle, cone angle, helix angle and profile-shift coefficient on the theoretical gear mesh is performed. The parametric analysis of pitch cone design shows that the dominant design parameters represented by the angle between the first principle directions (FPD) and normal angular factor are more sensitive to the shaft and cone angles than they are to the helix angle. The theoretical contact path is highly sensitive to the profile-shift coefficient, which is determined from the theoretical tooth contact analysis. The FPD angle is found to change the distribution of contact pattern, contact pressure and root stress as well as the translational transmission error and the variation of the mesh stiffness significantly. The contact pattern is clearly different between the drive and coast sides due to different designed FPD angles. Finally, a practical experimental setup for marine transmission is performed and tooth bearing test is conducted to demonstrate the proposed design procedure. The experimental result compared well with the simulation. Results of this study yield a better understanding of the geometry design and loaded gear mesh characteristics for crossed beveloid gears used in marine transmission.

Key words: beveloid gears, loaded tooth contact analysis, crossed axes, marine transmission

1 Introduction

Beveloid gears, first proposed by BEAM[1], are now widely applied in marine, low-backlash planetary and automotive transmissions[2–3]. A typical down angle type marine transmission installed in an extremely limited space for a speedboat with inclined output shaft is shown in Fig. 1. The system consists of an engine, a beveloid gearbox and a propeller. The beveloid gear used here is a type of an involute gear with an extremely general design with variable tooth thickness, roots and outside diameters over the tooth width. This type of design is suitable for power and motion transmission not only between parallel axes, but also between intersecting or crossed axes. However, the main weakness in crossed axis application is that the beveloid gear mesh is theoretically in point contact with a high sliding velocity. This unfavorable engagement behavior negatively affects the surface durability and causes harmful vibration and unwanted noise problems.

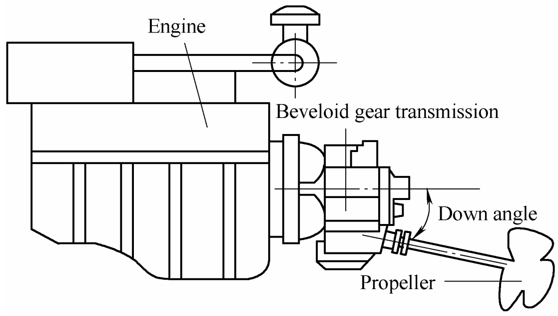

Fig. 1. Marine drive transmission with down angle

Recently, there has been some efforts made to widen the application of spatial beveloid gear drive[4–11]. MITOME[4–6], proposed three important manufacturing methods, which are the inclining work-arbor taper hobbing method, the table

* Corresponding author. E-mail: chaoshengsong@hotmail.com
This project is supported by Fundamental Research Funds for Central Universities of China (Grant No. CDJXS11111138, Key Projects in the National Science & Technology Pillar Program during the 11th Five-Year Plan Period of China(Grant No. 2011BAF09B07), and National Natural Science Foundatlon of China(Grant No. 51175523)

sliding taper hobbing method and the generating method by gear shaper. In addition, KOMATSUBARA, et al[7], performed analytical and experimental investigations on the influence of machine settings on the tooth contact behavior and developed a new concave-conical gearing for marine transmission with a better curvature relation at the contact points. TSAI, et al[8], proposed a new concept for designing skew conical gear drives, which are designed with approximate line contact by combining with profile-shifted transmission. LI, et al[9], proposed a new type of non-involute beveloid gear used for marine transmissions. ZHU, et al[10], analyzed the meshing characteristics of non-involute beveloid gears, and the results showed that the contact area can be increased through tooth end-relief and profile modification. HE and WU[11] developed a mathematical model based on the theory of gearing and performed theoretical tooth contact analysis to examine the meshing and bearing contact of involute gear with non-parallel axes. However, in spite of the above-mentionned studies, most of them are limited to geometry design, manufacturing analysis and preliminary tooth contact analysis. Very limited effort has been directed at studying the detailed effects of gearing parameters on the tooth contact behavior of crossed beveloid gears in marine transmissions with line contact. This paper attempts to bridge this gap in the literature.

This paper presents an analytical derivation of the geometry design procedure with line contact for a crossed beveloid gear pair. The relations between gearing parameters including the shaft angle, cone angle, helix angle and profile-shift coefficient, and the dominant geometry design parameter known as the first principle directions (FPD) angle is studied. Based on the proposed approach, the loaded tooth contact analysis using the finite element method is performed to investigate the salient features of crossed beveloid gears. Finally, an experimental setup was developed to validate the proposed design for marine transmission.

2 Crossed Axis Geometry Design

2.1 Line contact condition

The concept for designing beveloid gear drives is based on the gear-rack-model[8]. As shown in Fig. 2, each beveloid gear engages not only with each other but also with a "common rack" having zero thickness in line contact. The line $R-R$ represents the intersection between the pitch plane of the common rack and right tooth surface. In addition, K_1 and K_2 are the contact lines and ξ_{R1} and ξ_{R2} are the crossing angle between the contact lines and intersection line for the pinion and gear, respectively. The direction of observation is from the toe to the heel. An angle ξ is defined as the FPD angle.

Given the above setup, the crossing angle between K_1 and K_2 can be represented as follows:

$$\xi_{R(L)} = \xi_{R(L)1} + \xi_{R(L)2} \,. \tag{1}$$

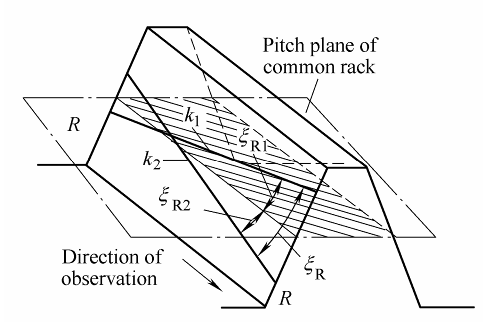

Fig. 2. Contact lines on the tooth surface of common rack

Fig. 3 shows the relation between the right tooth surface and the common rack. The contact line PA is the line between the gear and common rack. According to the involute gearing theory, the crossing angle between PA and the axis of the gear is the base helix angle β_{bR}. The line of intersection between plane axode and the tooth surface is PB. The crossing angle between PB and the axis of the gear is the working pitch helix angle β_{PwR}. The line of intersection between the pitch plane of the common rack and the tooth surface is PC, and r_ω is working pitch circle radius. Note that the plane of action is perpendicular to the transverse plane and the tooth surface.

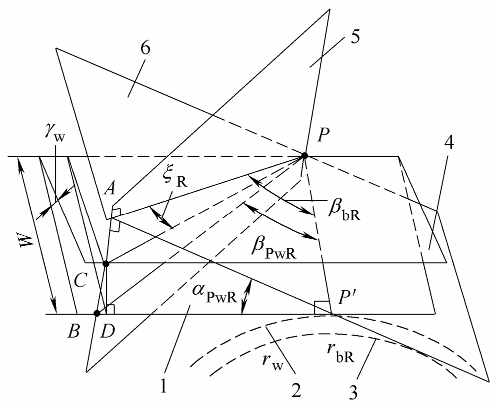

Fig. 3. Relations of tooth surface, pitch plane, plane axode and plane of action

1. Plane axode 2. Working pitch circle radius
3. Base circle radius 4. Pitch plane of the common rack
5. Tooth surface of the common rack 6. Plane of action

Accordingly, the following relation can be derived:

$$\tan\xi_R = \frac{AC}{PA} = \frac{AB-CB}{PA} \,. \tag{2}$$

Substituting the following equations:

$$\begin{cases} PA = W/\cos\beta_{bR}\,, \\ AB = W\tan\beta_{PwR}\sin\alpha_{PwR}\,, \\ BC = W\tan\gamma_w/\cos\alpha_{PwR}\,, \end{cases} \tag{3}$$

where $\alpha_{\rm pwR}$ is the working pressure angle of the right tooth and $\gamma_{\rm w}$ is the working cone angle, yields

$$\tan\xi_{\rm R}=\cos\beta_{\rm bR}\left(\tan\beta_{\rm PwR}\sin\alpha_{\rm PwR}-\frac{\tan\gamma_{\rm w}}{\cos\alpha_{\rm PwR}}\right). \quad (4)$$

By applying a set of trigonometric relations, the following equation can be obtained:

$$\tan\xi_{\rm R}=\frac{\tan\beta_{\rm PwR}\tan\alpha_{\rm PwR}-\tan\gamma_{\rm w}\left(1+\tan^2\alpha_{\rm PwR}\right)}{\sqrt{1+\tan^2\alpha_{\rm PwR}+\tan^2\beta_{\rm PwR}}}. \quad (5)$$

Then, from the relation between the reference gearing data and working gearing data[2], it can be shown that

$$\tan\alpha_{\rm PwR}+\tan\alpha_{\rm PwL}=2\frac{\tan\alpha_{\rm nw}\cos\gamma_{\rm w}}{\cos\beta_{\rm w}}, \quad (6)$$

$$\tan\beta_{\rm PwL}+\tan\beta_{\rm PwR}=2\tan\beta_{\rm w}\cos\gamma_{\rm w}, \quad (7)$$

where $\alpha_{\rm nw}$ is the working normal pressure angle, $\beta_{\rm w}$ is the working helix angle and $\gamma_{\rm w}$ is the working cone angle.

Subsequently, the following equations can be obtained for the right tooth:

$$\tan\xi_{\rm R}=\tan\beta_{\rm w}\sin\alpha_{nw}-\frac{\tan\gamma_{\rm w}\cos\alpha_{\rm nw}}{\cos\beta_{\rm w}}. \quad (8)$$

Similarly, for the left tooth,

$$\tan\xi_{\rm L}=\tan\beta_{\rm w}\sin\alpha_{\rm nw}+\frac{\tan\gamma_{\rm w}\cos\alpha_{\rm nw}}{\cos\beta_{\rm w}}. \quad (9)$$

Then, the approximate line contact condition can be represented as

$$\xi_{\rm L(R)1}+\xi_{\rm L(R)2}=\xi_{\rm L(R)}\approx 0. \quad (10)$$

Where subscripts L and R indicate the left and right teeth, respectively. Also, subscripts 1 and 2 indicate the pinion and gear, respectively.

2.2 Geometry design procedure

2.2.1 Beveloid gear meshing

According to the spatial involute gearing theory, the beveloid gear engages with the common rack. This implies that the following conditions should be satisfied[12]:

(1) The normal pitch of the common rack is equal to the normal base pitch of the beveloid gear;

(2) The transverse base circle pitch is equal to the base pitch (Normal pitch) of the beveloid gear.

The above two conditions can be represented mathematically as follows:

$$\pi m_{\rm nw}\cos\alpha_{\rm nw}=\pi m_{\rm n}\cos\alpha_{\rm n}, \quad (11)$$

$$\pi m_{\rm tw}\cos\alpha_{\rm PwL(R)}=\pi m_{\rm t}\cos\alpha_{\rm PL(R)}, \quad (12)$$

where $m_{\rm tw}=m_{\rm nw}/\cos\beta_{\rm w}$, $m_{\rm t}=m_{\rm n}/\cos\beta$, $m_{\rm n}$ is the normal module, $\alpha_{\rm n}$ is the normal pressure angle, $\alpha_{\rm pj}(j=\text{L, R})$ is the reference pressure angle, and β is the reference helix angle.

Then the working normal module and working pressure angle of the common rack cutter can be represented by

$$m_{\rm nw}=m_{\rm n}\frac{\cos\beta_{\rm w}}{\cos\beta}\frac{\cos\alpha_{\rm PL(R)}}{\cos\alpha_{\rm PwL(R)}}, \quad (13)$$

$$\cos\alpha_{\rm nw}=\xi_{\rm t}\cos\alpha_{\rm n}\frac{\cos\beta}{\cos\beta_{\rm w}}, \quad (14)$$

$$\frac{m_{\rm n}}{m_{\rm nw}}=\frac{\cos\alpha_{\rm nw}}{\cos\alpha_{\rm n}}=\xi_{\rm t1}\frac{\cos\beta_1}{\cos\beta_{\rm w1}}=\xi_{\rm t2}\frac{\cos\beta_2}{\cos\beta_{\rm w2}}=\xi_{\rm n}, \quad (15)$$

where $\xi_{ti}\left(i=1,2\right)$ is the transverse angular factor, $\xi_{\rm n}$ is the normal angular factor, and $r_{\rm p}$ is the reference pitch circle radius.

2.2.2 Working pitch cone design

Fig. 4 shows the relation of the working pitch cones of a crossed beveloid gear pair. From the derivation of the working pitch cone design, the shaft angle, offset and mounting distance can be represented by

$$d_1=-\frac{r_{\rm w2}}{\sin\gamma_{\rm w1}\cos\gamma_{\rm w2}}+\frac{E\left(\sin^2\delta-\sin^2\gamma_{\rm w1}-\sin^2\gamma_{\rm w1}\cos\delta\right)}{\sin\gamma_{\rm w1}\sin\delta\sqrt{\sin^2\delta-\sin^2\gamma_{\rm w1}-\sin^2\gamma_{\rm w2}-2\sin\gamma_{\rm w1}\sin\gamma_{\rm w2}\cos\delta}}, \quad (16)$$

$$d_2=\frac{r_{\rm w2}}{\sin\gamma_{\rm w2}\cos\gamma_{\rm w2}}-\frac{E\left(\sin\gamma_{\rm w1}\cos\delta+\sin^2\gamma_{\rm w2}\right)}{\sin\delta\sqrt{\sin^2\delta-\sin^2\gamma_{\rm w1}-\sin^2\gamma_{\rm w2}-2\sin\gamma_{\rm w1}\sin\gamma_{\rm w2}\cos\delta}}, \quad (17)$$

$$\cos\left(\beta_{w1}+\beta_{w2}\right)=\tan\gamma_{w1}\tan\gamma_{w2}+\frac{\cos\delta}{\cos\gamma_{w1}\cos\gamma_{w2}}, \quad (18)$$

$$E=\frac{\left(r_{w1}\cos\gamma_{w2}+r_{w2}\cos\gamma_{w1}\right)\sin\left(\beta_{w1}+\beta_{w2}\right)}{\sin\delta}, \quad (19)$$

where $d_i(i=1,\ 2)$ is the mounting distance, δ is the shaft angle, and E is the offset.

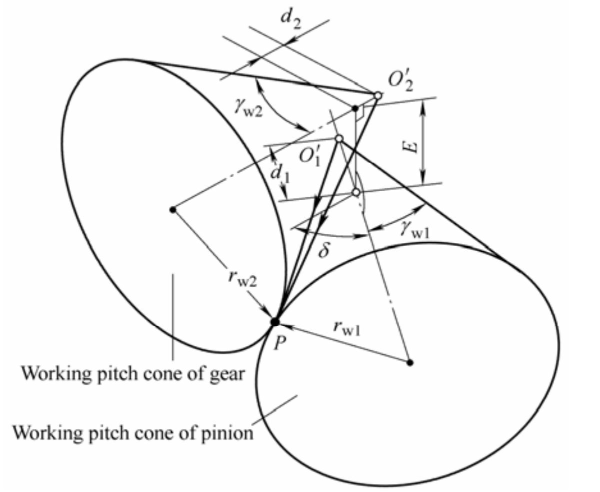

Fig. 4. Working pitch cones of beveloid gears

2.2.3 Backlash-free condition

A backlash-free condition is still necessary for the design of a beveloid gear pair having crossed axis. According to HE and WU[13], the backlash-free equation can be represented as follows:

$$2\tan\alpha_n\left(x_{t1}\frac{\cos\gamma_1}{\cos\beta_1}+x_{t2}\frac{\cos\gamma_2}{\cos\beta_2}\right)=$$
$$\frac{N_1}{2}\left(\text{inv}\alpha_{PwL1}+\text{inv}\alpha_{PwR1}-\text{inv}\alpha_{PL1}-\text{inv}\alpha_{PR1}\right)+$$
$$\frac{N_2}{2}\left(\text{inv}\alpha_{PwL2}+\text{inv}\alpha_{PwR2}-\text{inv}\alpha_{PL2}-\text{inv}\alpha_{PR2}\right), \quad (20)$$

where x_{t1} and x_{t2} are the profile-shift coefficients in the pinion and gear transverse sections, and $N$is the tooth number.

2.2.4 Line contact condition design

Fig. 5 illustrates the design procedure for the condition that the offset$E$ is given considering the line contact condition. The cone angleγ_1 is used as a cyclic variable and the normal angular factor ξ_n and helix angle β_2 are applied as two variables for simplifying the solution.

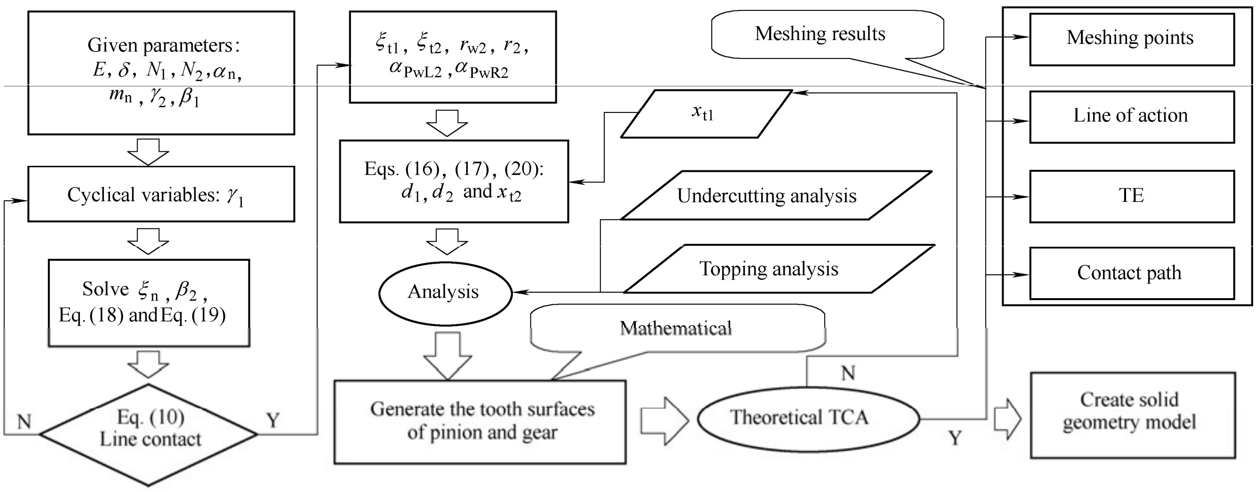

Fig. 5. Design procedure for line contact condition

To obtain the line contact solution, an iterative algorithm was used to solve the nonlinear relation as shown in Eqs. (18), (19). Note that the line contact condition of Eq. (10) is used to fix the cyclic variable. Then the pitch cone results given by Eqs. (16), (17) are used to calculate the working mounting distances d_1 and d_2. Assuming a profile-shift coefficient x_{t1}, the backlash free condition defined by Eq. (20) is used to obtain another profile-shift coefficient x_{t2}. Also, a specific analysis is performed here to avoid undercutting and topping. Then the coordinates of the points on tooth surface of pinion and gear can be obtained by means of the simulation of manufacturing. Theoretical tooth contact analysis is conducted to get the meshing results including meshing points, line of action,transmission error (TE) and contact path. Through the analysis of the contact path on the tooth surface, the profile-shift coefficient x_{t1} can be determined. The solid geometry model is subsequently created applying the known mathematical coordinates.

3. Parametric and Tooth Contact Analysis

3.1 Influence of gearing parameters

Since angle $\xi_{L(R)}$ between the first principle directions (FPD) and ξ_n normal angular factor are the dominant geometry parameter for crossed beveloid gear design assuming line contact, the influences of gearing parameters on them are studied next. Also, the effect of profile-shift coefficient on contact path is examined. Fig. 6 shows the effect of the variation of cone angle on FPD angle for cases with different shaft angles. It is assumed that the gear pair has the same offset, helix angle of pinion, normal module and normal pressure angle. The result indicates a strong incremental relation between the FPD angle $\xi_{L(R)}$ and the shaft angle. However, the trends for ξ_R and ξ_L are different as the cone angle of pinion γ_1 increases, because ξ_R is degressive and ξ_L is incremental. Also, when the cone angle γ_1 is fixed, the increase of one angle γ_2 has a degressive effect on ξ_R and increasing effect on ξ_L as shown in Fig. 6 (b).

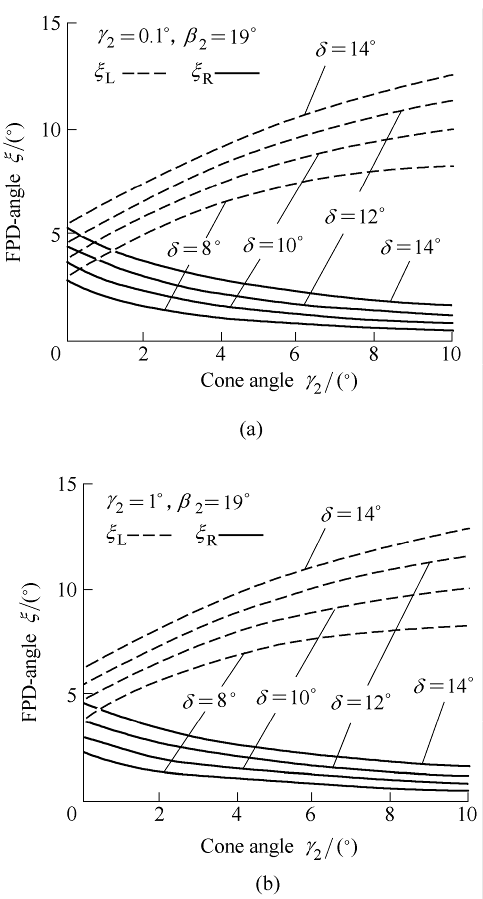

Fig. 6. Influence of cone angle on FPD angle

As shown in Fig. 7 (a), the normal angular factor ξ_n tends to decrease when the cone angle increases for different shaft angles. When the cone angle is less than 2°, the values of normal factor for different shaft angle are similar. However, when the cone angle is larger than 2°, the normal angular factor ξ_n becomes smaller as the cone angle of pinion increase. Also, the similar trend exists when shaft angle δ decreases. Assuming that the cone angle γ_1 is fixed, the effect on the normal angular factor is not obvious for different values of cone angle γ_2 as shown in Fig. 7 (b). As shown in Fig. 8 (a), the FPD angles are parabolic in shape and therefore the helix angle β_1 has less influence on the FPD angle. However, for different shaft angles, higher value of FPD angle is obtained with higher shaft angle. In Fig. 8 (b), when the cone angle γ_1 is fixed, the increase of cone angle γ_2 leads to an increased FPD angle ξ_L and a decreased in the other FPD angle ξ_R. The analysis results show that helix angle has less influence on FPD angle compared to the cone angle. The results in Fig. 9 indicate that the helix angle β_1 has a significant influence on normal angular factor ξ_n. With increasing the helix angle β_1, the normal angular factor decreases initially and then increases.

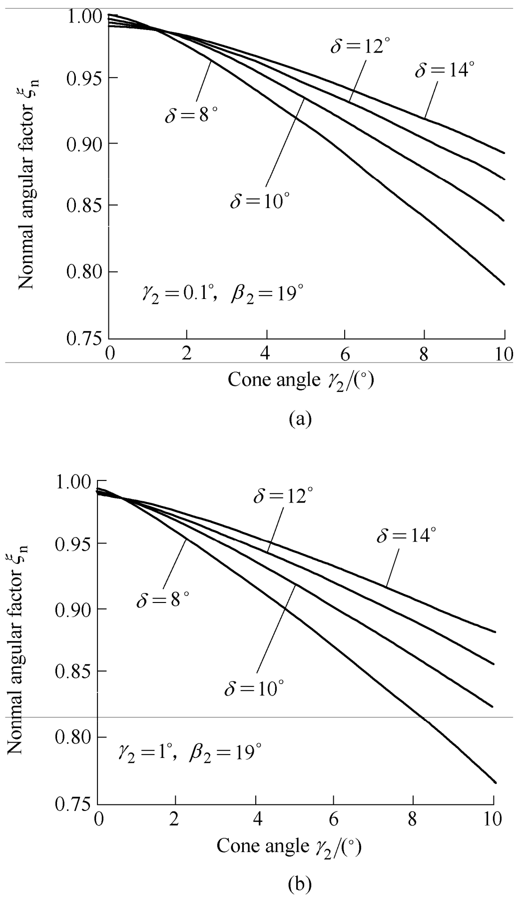

Fig. 7. Influence of cone angle on normal angular factor

Using the mathematical model of tooth surface of beveloid gear, a theoretical mesh model was setup and a theoretical tooth contact analysis was performed. As illustrated in Figs. 10(a)–10(d), the profile-shift coefficient x_t has a strong influence on the contact path. With the decrease of x_{t1} from 0.2 to 0.1, the position of contact path on tooth surface changes from the toe to the heel for the pinion, and from the heel to the toe for the gear. In order to obtain a high quality engagement between the pinion and gear, the profile-shift coefficient should be determined carefully according to the simulation results from theoretical tooth contact analysis (TCA).

3.2 Loaded tooth contact analysis

A quasi-static loaded tooth mesh model for the crossed beveloid gear is analyzed by a 3-dimensional tooth contact analysis program[14] to obtain the effective mesh point, line-of-action, mesh stiffness and static transmission error. The specialized TCA program employs a hybrid finite element-analytical mechanics approach to simulate the physics of tooth engagement[15]. The schematic for the loaded mesh model of the crossed beveloid gear pair is illustrated in Fig. 11(a).

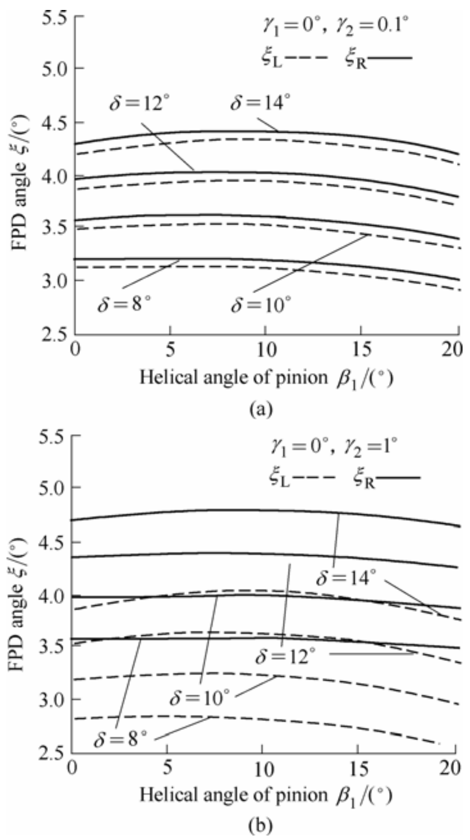

Fig. 8. Influence of helix angle of pinion on FPD angle

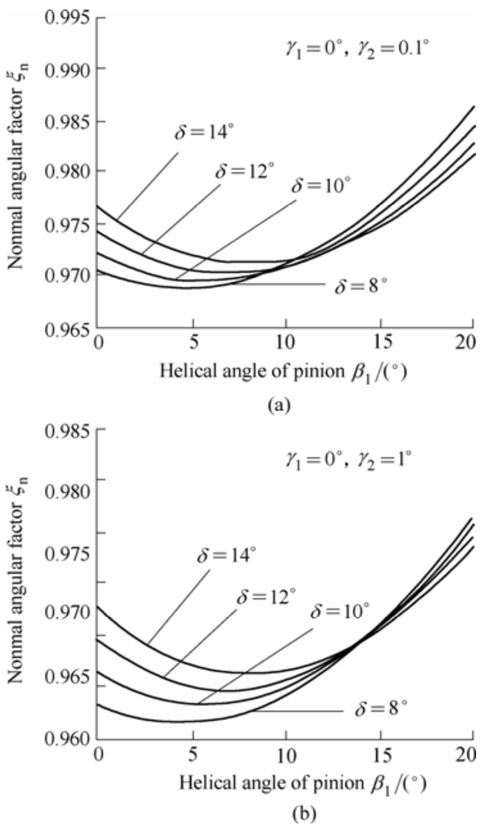

Fig. 9. Influence of helix angle of pinion on normal angular factor

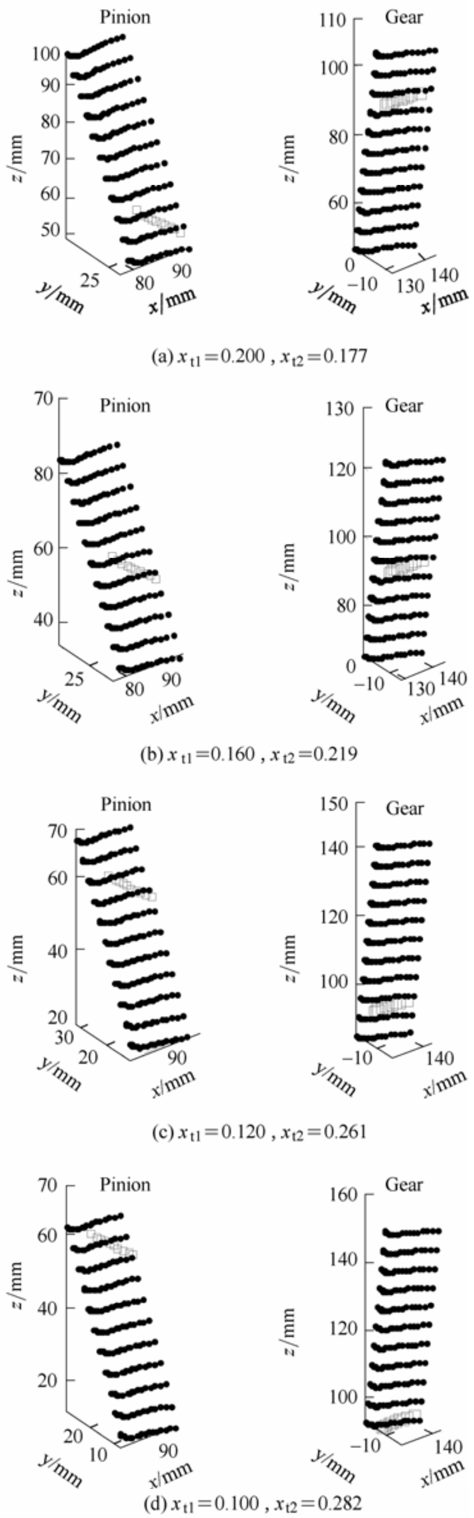

Fig.10. Influence of profile-shift coefficient on contact path

As shown in Fig. 11 (b), $S_1(x_1, y_1, z_1)$ and $S_2(x_2, y_2, z_2)$ are the coordinate systems fixed to the pinion and gear, respectively. In addition, $S_f(x_f, y_f, z_f)$ is fixed to the frame as the global coordinate system. The label *P* represents the meshing point. Four cases with different FPD angles are analyzed for the proposed beveloid gear drive in line contact. The fundamental design parameters are listed in Table 1 and the gearing data are listed in Table 2. The tooth meshing characteristics on both the drive and the coast sides are examined here.

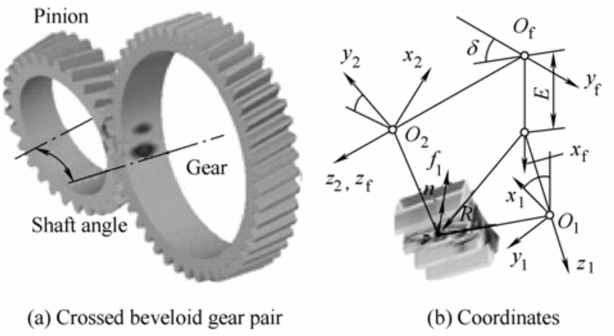

Fig. 11. Assembly and coordinate systems for the beveloid gear pair model

Table 1. Fundamental design parameters

Symbol	Pinion (Beveloid)	Gear (Beveloid)
Normal module m_n/mm	6	
Normal pressure angle α_n/(°)	20	
Number of teeth N	29	45
shaft angle δ/(°)	13	
Offset E/mm	229	

Table 2. Gearing data for loaded tooth contact analysis

Symbol	Case 01		Case 02		Case 03		Case 04	
	Pinion	Gear	Pinion	Gear	Pinion	Gear	Pinion	Gear
Cone angle γ/(°)	3.0	1.0	2.0	0.8	1.0	0.8	0.4	0.2
Helix angle β/(°)	25	–12.71	23	–10.38	20	–7.24	22	–9.11
Profile shifting factor x_t	0.29	0.368 2	0.15	0.192 7	0.16	0.219 1	0.12	0.15
Normal angular factor ξ_n	0.985 1		0.991 8		0.990 8		0.993 4	
FPD angle ξ_R/(°)	1.660 0		2.408 1		3.351 1		4.439 9	
FPD angle ξ_L/(°)	8.750 6		7.570 2		6.581 5		5.552 2	

Fig. 12 shows the contact pattern on both the drive side and coast side under a medium load (300 N • m) for four cases. It is clear that the beveloid gears engage with each other in line contact and the contact patterns are all approximately located in the middle of the tooth surfaces.The contact area on the drive side and coast side are different due to different designed FPD angles. Also, the area of the contact pattern drops from approximately 90% to approximately 35% of the tooth surface due to the increase of FPD angle from 1.660° to 4.439°. This result agrees with the practical application of the FPD angle.

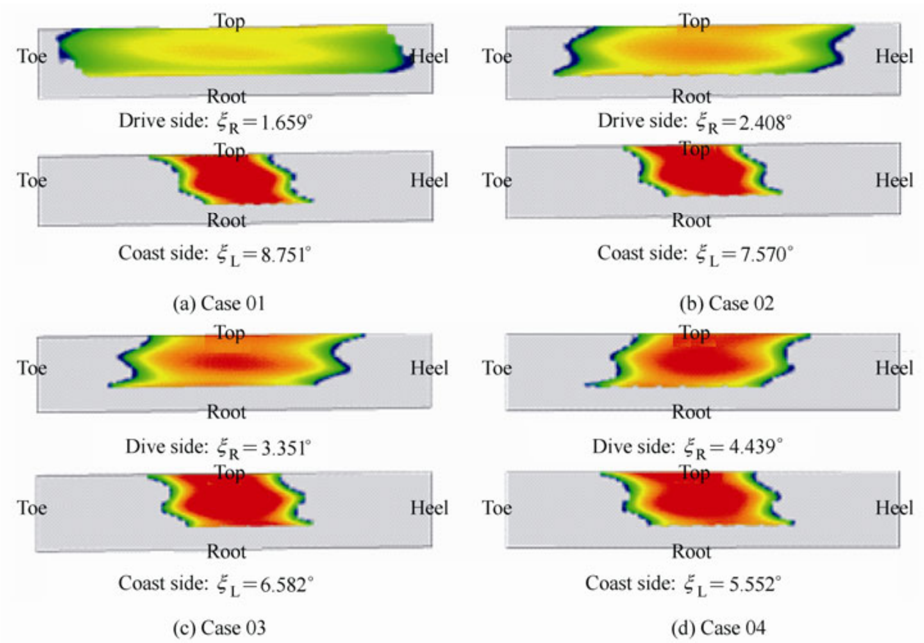

Fig. 12. Influence of FPD angle on loaded tooth contact pattern

The distribution of contact pressure over the engaged tooth surface in a typical parabolic shape is illustrated in Fig. 13. The calculated results show that higher designed FPD angle tends to cause higher peak value of contact pressure due to lesser area coming into contact. For the mesh stiffness as shown in Fig. 14, it is obviously parabolic in shape. Since less area comes into contact with the increase in FPD angle at the same load level, the average value of mesh stiffness decreases. This result agrees with intuition and seems reasonable. The distribution of the root stress along the profile direction and the tooth width direction is shown in Fig. 15 (a) –15(b).

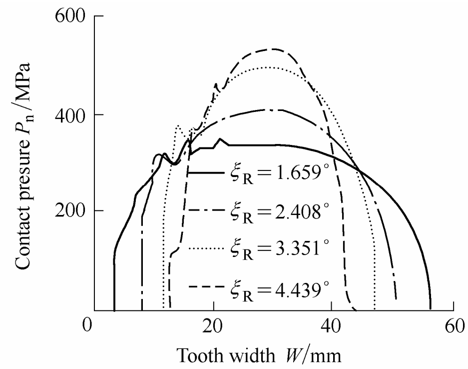

Fig. 13. Influence of FPD angle on contact pressure

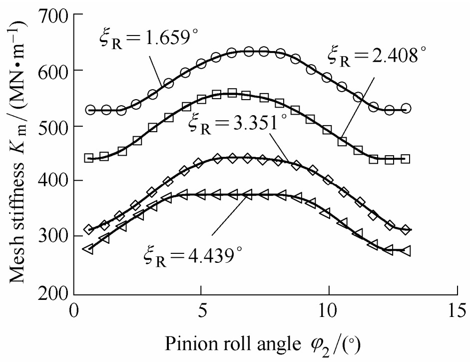

Fig. 14. Influence of FPD angle on mesh stiffness

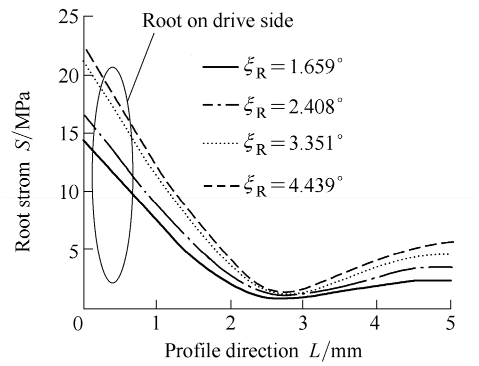

(a) Profile direction

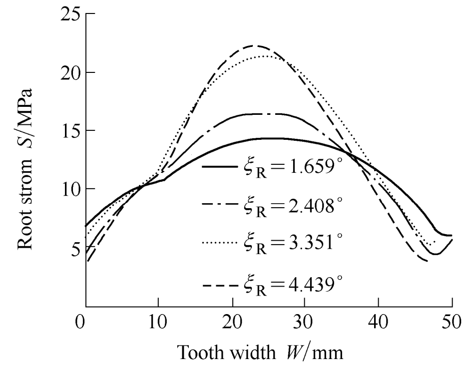

(b) Tooth width direction

Fig. 15. Influence of FPD angle on root stress

For the profile direction, the maximum value of root stress occurs at the tooth root fillet of drive side. Also, the increase of the designed FPD angle leads to the increase of the root stress since less area comes into contact causing higher contact pressure.

For the tooth width direction, the shape of root stress is similar to the parabolic shape of mesh stiffness. With the decrease of the FPD angle, the maximum value of root stress along the tooth width direction, which is located in the middle of face width, becomes lower. However, the shape of the root stress becomes flat, which agrees well with the contact pattern results.

The time-varying and peak-peak value of translational transmission error (LTE) along the line of action (LOA) in one mesh cycle for the FPD angles of interest are presented in Fig. 16(a)–16(b), respectively. It can be seen that the LTE is parabolic in shape and the FPD angle significantly changes the shape of the LTE function, which is similar to the effect on mesh stiffness. With decreasing FPD angle, the LTE flattens and the peak-to-peak value of LTE that essentially excites vibration decreases due to more area coming into contact. The detailed mesh parameters are listed in Table 3.

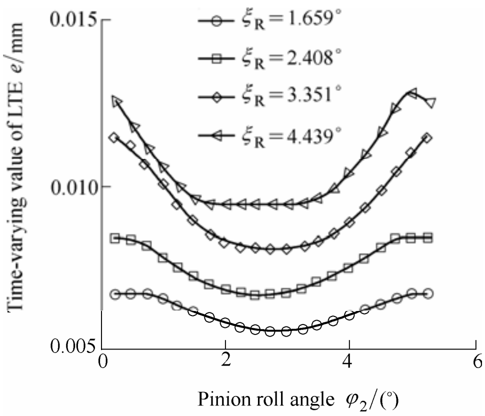

(a) Time-varying value along line-of-action

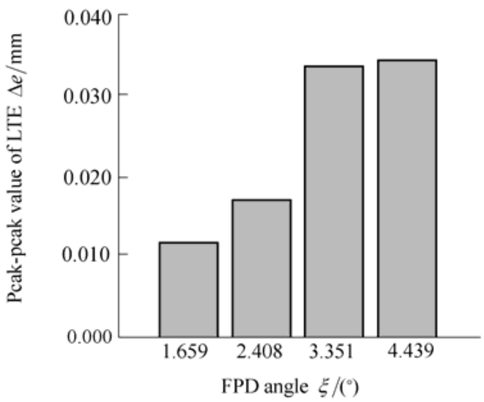

(b) Peak-peak Value

Fig. 16. Influence of FPD angle on translational transmission error

Table 3. Average mesh parameters for different FPD-angle

FPD-angle ξ_R /(°)	Mesh Point P/m Line-of-action n	LTE e/m	Mesh stiff. K_m/(MN · m^{-1})
1.659	(0.095, 0.027, –0.148) (–0.114, –0.902, 0.414)	0.006	574.7
2.408	(0.095, 0.018, –0.093) (–0.170, –0.909, 0.378)	0.007	495.6
3.351	(0.094, 0.011, –0.058) (–0.244, –0.912, 0.327)	0.009	385.8
4.439	(0.095, 0.003, –0.048) (–0.318, –0.879, 0.354)	0.010	340.0

4 Experimental Study

An experimental setup demonstrating the application of the proposed design procedure for a marine transmission is perfomed. A test rig was established for beveloid gearbox as shown in Fig. 17. The conventional hobbing method was used to generate the crossed beveloid gear set using the gearing data of case03 as shown in Fig. 18. A medium load (300 Nm) condition was applied and the contact patterns was measured. As shown in Fig. 19, it is obvious that the beveloid pinion engaged with the beveloid gear in line contact and that the contact area reaches about 65 per cent of the right tooth surface of the gear, which compares well with the simulation results as shown in Fig. 12 (c).

Fig. 17. Experimental setup for crossed beveloid gears used in marine transmission

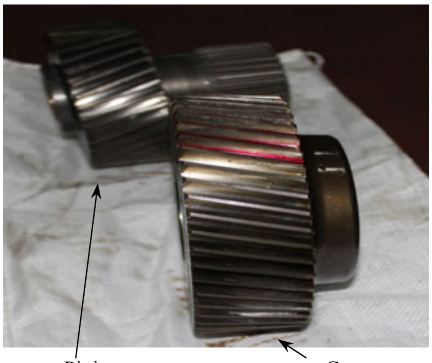

Fig. 18. Test beveloid gears

Fig. 19. Contact pattern of right tooth surface

5 Conclusions

(1) The shaft and cone angle have a strong effect on the first principle directions FPD angle. On the other hand, the helix angle has less effect. The contact path is very sensitive to the profile-shift coefficient, which should be determined carefully through the theoretical tooth contact analysis.

(2) The loaded meshing characteristics including loaded contact pattern, contact pressure, root stress, mesh stiffness and translational transmission error are very sensitive to the dominant FPD angle design parameter. The contact pattern is clearly different between the drive and the coast sides due to different designed FPD angles.

(3) The tested beveloid gears show an area of contact pattern that reaches 65 percent of the total tooth surface, which compares very well with the simulated results.

References

[1] BEAM A S. Beveloid gearing[J]. *Mach. Des.*, 1954, 26(2): 220–238.

[2] BORNER J, HUMM K, JOACHIM F, et al. Application, design, and manufacturing of conical involute gears for power transmissions[J]. *VDI BERICHTE*, 2005, 1904(1): 125–144.

[3] KOMATSUBARA H, MITOME K, OHMACHI T, et al. Development of concave conical gear used for marine transmissions (1st Report, Principle of Generating Helical Concave Conical Gear) [J]. *JSME International Journal*, *Series C*, 2002, 45(1): 371–377.

[4] MITOME K. Table sliding taper hobbing of conical gear using cylindrical hob, part 1: theoretical analysis of table sliding taper hobbing[J]. *Transactions of the ASME*, 1981, 103(4): 446–451.

[5] MITOME K. Table sliding taper hobbing of conical gear using cylindrical hob, part 2: hobbing of conical involute gear[J]. *Transactions of the ASME*, 1981, 103(4): 542–455.

[6] KIKUCHI T, MITOME K, OHMACHI T. Cutting method of concave conical gear by gear shaper(1st report, theory of general tooth surface)[J]. *Transactions of the Japan Society of Mechanical Engineers*, *Part C*, 2004, 70(693): 1 470–1 475.

[7] KOMATSUBARA H, MITOME K, OHMACHI T, et al. Development of concave conical gear used for marine transmissions (2nd report, principle of generating helical concave conical gear) [J]. *JSME International Journal*, *Series C*, 2002, 45(2): 543–550.

[8] WU S H, TSAI S J. Geometrical design of skew conical involute gear drives in approximate line contact[J]. *Proceedings of the Institution of Mechanical Engineers*, *Part C*, *Journal of Mechanical Engineering Science*, 2009, 223(9): 2 201–2 211.

[9] LI G X, WEN J M, ZHANG X, et al. Meshing theory and simulation of noninvolute beveloid gears[J]. *Mechanism and Machine Theory*, 2004, 39(8): 883–892.

[10] ZHU C C, WANG H X, ZHANG L, et al. Contact characteristics of helical conical gears used for V-drive marine transmissions[J]. *Proceedings of the Institution of Mechanical Engineers*, *Part C*, *Journal of Mechanical Engineering Science*, 2011, 225(1): 216–224.

[11] HE J L, WU X T. Tooth contact analysis of conical involute gears[J]. *Chinese Journal of Mechanical Engineering*, 2006, 19(1): 105–108.

[12] LI H M, Han Yuanying, Wang Zhixing. *Geometric principle and calculation of involute gears* [M]. Beijing: China Machine Press, 1985: 263–299.

[13] HE J L, WU X T. Study on geometry of conical involute gear pair with nonintersecting-nonparallel-axes[J]. *Journal of Xi'an Jiatong University*, May, 2003, 37(5): 471–474.

[14] VIJAYAKAR S. Contact analysis program package: HypoidK[CP]. *Advanced Numerical Solutions*, Hilliard, Ohio, USA, 2009.
[15] VIJAYAKAR S. *Finite element methods for quasi-prismatic bodies with application to gears*[D]. Columbus, Ohio: The Ohio State University, 1987.

Biographical notes

ZHU Caichao, born in 1967, is currently a professor and a PhD candidate supervisor at *State Key Laboratory of Mechanical Transmission, Chongqing University, China*. He received his PhD degree from *Chongqing University, China*, in 1998. His research interests include design and dynamics of precision machine elements, gear noise and vibration control.
Tel: +86-23-65111192; E-mail: cczhu@cqu.edu.cn

SONG Chaosheng, born in 1983, is currently a PhD candidate at *State Key Laboratory of Mechanical Transmission, Chongqing University, China*. He received his master degree on mechanical design and theory in *Chongqing University, China*, in 2007. He spent one year as a visiting scholar at *University of Cincinnati* to conduct research in gear design and gear dynamics. His research interests include design and dynamics of beveloid geared rotor system.
Tel: +86-23-65111192; E-mail: chaoshengsong@hotmail.com

LIM Teik Chin, born in 1965, is currently the Herman Schneider Professor of mechanical engineering and director of *School of Dynamic Systems at University of Cincinnati, Ohio, USA*. Also, since 2008, he holds the Chang Jiang Chair Professorship at *Chongqing University of China*. He received his PhD degree in mechanical engineering from *the Ohio State University, USA*, in 1989. His research interests include gear noise and vibrations, structural vibrations and acoustics, active noise and vibration control, automotive NVH (noise, vibration & harshness) and product sound quality design.
Tel: +01-513-556-4450; E-mail: teik.lim@uc.edu

VIJAYAKAR Sandeep, is currently the owner and Chief Technical Officer of *Advanced Numerical Solutions (ANSOL), Ohio, USA*. He has developed finite element and contact mechanics models and programs for analyzing response of rotating gears and bearings. He received the PhD in mechanical engineering from *the Ohio State University, USA*, in 1987. His research interests include contact mechanics, finite elements, gear design, gear dynamics and advanced numerical algorithms.
Tel: +01-614-771-4861, E-mail: sandeep@ansol.com